Mesospheric Odd Nitrogen Enhancements During Relativistic Electron Precipitation Events

A. C. Aikin
Laboratory for Atmospheres
Goddard Space Flight Center
Greenbelt, MD 20771

H. J. P. Smith
TPE Associates
Chestnut Hill, MA 02467

Abstract

The behavior of mesospheric odd nitrogen species during and following relativistic and diffuse auroral precipitation events is simulated, Below 75 km nitric oxide is enhanced in proportion to the ion pair production function associated with the electron precipitation and the length of the event. Nitrogen dioxide and nitric acid are also enhanced. At 65 km the percentage of odd nitrogen for N is 0.1%, HNO_3 is 1.6%, NO_2 is 15%, and NO is 83.3%. Between 75 and 85 km NO is depleted during particle events due to the faster destruction of NO by N relative to the production of NO by N reacting with O_2. Recovery of NO depends on transport from the lower thermosphere, where NO is produced in abundant amounts during particle events.

Introduction

When no precipitating electrons are present, most mesospheric nitric oxide originates from ion-molecule reactions in the lower thermosphere and NO is subsequently transported into the mesosphere. There are small local sources of NO produced by galactic cosmic radiation and the reaction of any remaining N_2O with $O(^1D)$. Estimates of thermospheric NO production using normal gas phase chemistry in conjunction with ion-molecule reactions underestimate NO. This occurs in spite of including excited $N(^2D)$ and hot ground state $N(^4S)$ atoms to enhance the production of NO in the reaction with O_2 to produce NO. Recent studies by Swaminathan et al. [1998] indicate that including hot N, produced by photoelectrons from solar x-ray ionization of air was insufficient to account for the observed thermospheric NO.

Energetic electron and proton particle precipitation into the mesosphere produces N_2^+ by direct ionization and N^+ by disociative ionization. Secondary electrons associated with ionization produce N in both the ground and ^2D states. Reactions involving these products produce NO [Rusch et al., 1981]. It is expected that there will be a near term enhancement in mesospheric NO associated with the direct particle precipitation. This will be in advance of any enhancement associated with NO transported from the thermosphere, where it may be produced by charged particle bombardment.

Since odd nitrogen is very important as a catalytic loss component of stratospheric odd oxygen, considerable effort has been devoted to identifying all sources of odd nitrogen, see for example Vitt and Jackman, [1996]. Mesospheric nitric oxide has a lifetime sufficiently long to allow it to be transported into the stratosphere. It has been suggested that the fluxes are large enough to have a significant effect on the stratospheric odd nitrogen budget, [Callis et al., 1998]. It is well established that in winter there is strong air mass descent throughout the middle atmosphere at high latitudes resulting in the transport of nitric oxide from the upper stratosphere into the lower stratosphere and the transport of mesospheric NO into the upper stratosphere. One potential problem with quantitative estimates of the magnitude of this process is the assumption that all ionization leads to the formation of NO at the rate of one molecule per 1.2 to 1.6 ion pairs per $cm^{-3}s^{-1}$. Since detailed ion and neutral chemistry is involved, this assumption may not always be true particularly in the mesosphere. This paper includes details of the chemistry used to compute the expected mesospheric NO distribution for a range of particle fluxes and energy spectra. In addition to protons from solar flares and electrons associated with the aurora, there are a number of electron precipitation events occurring at lower latitudes and featuring hard electron spectra with

particles in the meV energy range [Rosenberg et al., 1972; Baker et al., 1987; Gains et al., 1995; and Frahm et al., 1997].

Mesospheric Ionization Events

Energetic charged particle ionization of the mesosphere consists of the long-term galactic cosmic ray source, protons from solar flares and electron precipitation events. In addition to aurora zone electron precipitation in the 1 to 200 Kev range, there are electron events termed diffuse aurora [Frahm et al., 1997]. There are also events lasting for as long as 10 days with energies as great as 1 to 2 meV. Such events are detected outside the auroral zone at lower L values. A well documented example is the event lasting from 10 to 22 May 1992 [Gaines et al., 1995]. In the calculations presented here representative ionization rates for these two types of events will be employed. In addition galactic cosmic radiation is included for the latitude representative of 70°N. The ionization rates are summarized in Table I.

Table I

Electron Ionization Rates cm^3s^{-1}

Alt/ Km	Hi Ionization	Lo Ionization
60	1e02	8e01
70	8e02	5e01
80	1e04	2e01

The Model and Its Initial Conditions

The HALOE solar occultation experiment on the UARS measures NO in the mesosphere and lower thermosphere. Although it was in position to observe northern high and midlatitudes at the beginning of May 1992, by the time of the 20 May particle event observations were being carried out from low latitudes where there were no significant atmospheric particle effects. The nitric oxide distribution originates as the result of transport from the lower thermosphere, where NO originates from solar x-ray ionization of the atmosphere [Swaminathan et al., 1998] and incoming fluxes of auroral electrons.

Initial neutral species concentrations were determined by a 2-D model with complete neutral chemistry and transport in the vertical and meridional planes [Jackman, private communication]. The diurnal time behavior was computed using a time-dependent box model, which included complete neutral and ion chemistry. The model operates with 249 reactions and 70 species of neutrals, positive and negative ions and electrons. The effect of dynamics is neglected in these computations. In the 60 to 80 km altitude regime the time constant for chemical processes is in most cases shorter than time constants associated with vertical and horizontal transport.

Mesospheric Nitrogen Chemistry of Ionization Events

Changes in mesospheric composition in response to ionization by energetic charged particles involve both neutral and ion chemistry. Air ionization results in the production N, O, H, OH, N_2^+, O_2^+, O^+, N^+ and electrons, e. Neutral and ion chemistry transfers these primary ionization products into other ion species, negative ions, various odd nitrogen species and modifies the distribution of ozone and odd hydrogen species. The odd nitrogen interactions are illustrated in Figure 1 (a modification of a figure by Scheibe [1979]). Ozone is affected most by odd hydrogen. The effect of these particle events on ozone has been treated elsewhere [Aikin and Smith, 1999]. Rate coefficients for all these processes have been taken from a variety of sources. Neutral chemistry rates are taken from the NASA chemical kinetic data survey [DeMore, 1997]. Some ion rates are taken from Zinn and Sutherland, [1990].Swaminathan et al.[1998] is also used as a source.

There have been several assessments of the amount and form of odd N produced per ion pair. Studies of electron deposition in N_2 with O_2 indicated that in addition to the ions N_2^+ and N^+ that $N(^2D)$ is produced [Green et al., 1984]. Calculations have shown that for every ion pair 0.67 N^+ and N_2^+ will be produced [Porter et al., 1979]. At least 0.5 $N(^2D)$ will be produced per ion pair. In studies of mesospheric odd nitrogen concentration changes during a solar flare proton event Rusch, et al., [1981] assumed that 0.88N per ion pair is produced in the ^2D state. In the present calculations the proportions allocated to the different N products of the ionization is in line with that given by Porter et al., [1979].

Dissociative recombination of N_2^+ can lead to $2N(^2D)$. However, there is usually charge exchange with O_2^+ through the fast ion-molecule reaction

$$N_2^+ + O_2 \rightarrow O_2^+ + N_2$$

This process eliminates as much as 50% of the production of NO by the ion pairs produced in the ionization process. In a similar manner N^+ charge exchanges with O_2

$$N^+ + O_2 \rightarrow N + O_2^+$$

leading to N divided in the proportions ^4S state 0.7 and in the ^2D state 0.3 [O'Keefe et al, 1986]. There is also production of NO^+ as another branch of this reaction. Dissociative recombination of NO^+ with an electron produces N in the ^4S state.

The primary mesospheric reactions linking N and NO are

$$N + O_2 \rightarrow NO + O$$

and

$$N + NO \rightarrow O + N_2 .$$

In this scheme N acts both to produce and destroy NO. When N is in the ^4S state, the reaction of N with O_2 for NO formation is slow. The reaction of N with NO is fast. As a result the production of large amounts of N during particle events does not lead to as much NO as might be expected. In fact there may be a decrease in the NO concentration at altitudes above 70 km unless N is in the ^2D state. Under these conditions the reaction of $N(^2D)$ with O_2 to produce NO is fast leading to more NO. Another source of $N(^2D)$ may be needed. In the normal mesosphere there is no significant source of N to produce NO and it must be transported from the lower thermosphere, where it is produced by photoelectrons and ion-molecule reactions .

In addition to being destroyed by reacting with O_2, $N(^2D)$ reacts with H_2O This reaction has recently been studied in the laboratory and found to occur rapidly [Umemoto, et al., 1999].The observed product of the reaction is NH. OH can be produced indirectly from the reaction between $N(^2D)$ and H_2O. The primary loss of NH will be in the reaction with O_2

$$NH + O_2 \rightarrow NO + OH .$$

However, there is insufficient water in the mesosphere for this reaction to be effective as a loss process for $N(^2D)$.

Response of Mesospheric Odd Nitrogen to Particle Inputs

Three cases were investigated. In the first or CRB case no energetic particles other than background cosmic radiation is considered. This case simulates the undisturbed mesosphere. Particle results will be compared with this case. The second case uses particle input representative of the 20 May 1992 event. This is referred to as the low ionization case. The third case uses particle input representative of the diffuse aurora. Examples were calculated in which particles were imposed at the same flux for a period of 48 hours. This was followed by 24 hours of no particles at 65 and 70 km. At 75 km the time without particles is extended to 4 days. For the 80 km case the time without particles is 8 days. This allows an estimate of the buildup of odd nitrogen species and the subsequent decay in order to demonstrate the photochemical lifetime. Time begins at local noon in the figures displaying the temporal behavior of different constituents.

Nitric oxide During Ionization Events

Panels a of Figures 2 and 3 present the diurnal change in nitric oxide at altitudes of 65 and 70 km respectively. The time scale is hours from local noon, when the particles are first applied. In Figures 4 and 5, panel b, NO is plotted as a function of time. The time scales in these figures are days from the local noon when particles wee first applied, 6 days for 75 km and

10 days for 80 km. The no particle situation is the dotted curve. Ionization due to the low ionization case is illustrated by the dashed curve. In the solid curve the response to the high relativistic electron event is plotted. The no particle nitric oxide distribution in the mesosphere is characterized by a diurnal variation at altitudes at 75 km and lower altitudes. There is almost no diurnal changes at 80 km. The largest NO concentrations occur during the day. This follows from the interchange between NO_2 and NO, which occurs as the result of NO_2 photodissociation.

The nitric oxide diurnal variation at 65 km (panel b of Figure 2) is a factor of 3.5 for no ionization and nearly the same with particles. There is an abrupt increase at sunrise and a gradual decrease at sunset. Changes in water concentration have very little effect. Nitric oxide increases as long as particles are present. For the low ionization case the increase after 48 hours amounts to a factor of 150. For the high ionization case the increase is a factor of 200. The final 24 hours, when particles are not present, shows little decay in NO. At 70 km (panel b of Figure 3) the diurnal variation in the absence of particles is nearly a factor of 2. In the presence of particles there is less than a factor of 2 between day and night. The low ionization case increases NO by a factor of 2 after 2 days. The high ionization case gives a factor of 4 increase for NO at the end of 48 hours. There is no decay of NO during the day-long period when particles are not present.

Particle effects at 75 km (panel b of Figure 4) initially increase NO by 17% for the high ionization case. This enhancement occurs within the first hour of particle bombardment. Following this initial increase there is a decay of 30%. The NO remains nearly constant until particles are no longer present. When particles are removed the NO decreases another 30% so that the total NO loss is about 60%. Following a very small initial increase, nitric oxide decays for the entire period that particles are present. There is a further decay after particles are removed. The total loss of NO amounts to a factor of 3. The completness of NO destruction is studied by extending the calculation period with no particles from 1 day to 4 days. At the end of that time the NO density at 75 km has not changed from its value at the end of 24 hours after the cessation of incoming particles. For the 20 May particle event. nitric oxide decreases by a factor of 1.3 during the particle bombardment. With the end of particle input nitric oxide remains constant.

At 80 km (panel b of Figure 5) the destruction of NO with lowionization parrticles is nearly a factor of 2 during the particle event with no recovery after particle flux ceases. For the high partiocle flux case the NO decreases by a factor of 66. With the end of particles there is a further decrease in NO by a factor of nearly 3. Extending the no particle situation another 3 days does not result in NO recovery.

Atomic Nitrogen Variations

Atomic nitrogen concentrations increase with increasing ionization flux. Since the ionizing flux increases with altitude the N concentration does the same. This is illustrated in Figures 2 and 3, panels b, and Figures 4 and 5, panels a. There are common features at all altitudes; the rate at which N increases after the onset of particles and the decay rate once particles have been removed. There is insufficient N, NO, or NO_2 at any of the altitudes considered here to change the N loss rate compared to the loss with O_2. At altitudes above 65 km N increases by several orders of magnitude during the particle event. At 70 km the N concentration has a peak value of 10^6 cm^{-3} for an ionization rate of $8x10^2$ cm^3s^{-1} and a concentration of 10^5 cm^{-3} for an ionization rate of 50 cm^3s^{-1} so that the N concentration is proportional to the ionization rate. At 80 km the high ionization case of $1x10^4$ cm^3s^{-1} leads to $2x10^8$ cm^{-3} while an ionization rate of 20 cm^3s^{-1} yields $1x10^5$ cm^{-3}. A factor of 500 increase in ionization leads to a change in the N concentration by a factor of $2x10^3$. This indicates that more N remains in the atmosphere as the altitude increases. This follows from the loss rate for N being primarily due to its reaction with O_2 to form NO. As altitude increases the O_2 concentration falls. This conclusion is supported by examination of the decay curves for N after particles are removed. Below 70 km the decay time for 1/e is minutes. At 75 km and above the decay time is hours as can be seen by examining the curves in parts a of Figures 4 and 5. At 75 and 80 km the time without particles was extended from 1 day to 4 days. For 75 km N decays to its preparticle value within one day after particles have been discontinued. In the low ionization case at 75 km N decays to the preionization value in half a day. With the high ionization rate N has not decayed to the preionization value. Nine days after the particles have been turned off there is still enhanced N by several orders of magnitude.

Nitrogen Dioxide Variation

Nitrogen dioxide exhibits a strong diurnal variation at all altitudes. At 65 km the variation is 3 orders of magnitude. This change is independent of ionization rate. Figure 6a illustrates the diurnal change at 65 km. After 24 hours of strong particle flux NO_2 has increased by a factor of 50. The weaker particle spectrum enhances the NO_2 by a factor of 20 in the same time period. At 70 km the diurnal change for no particles is $4x10^3$. For the weak particle flux the diurnal change is $3x10^3$ and the strong particle flux case gives 1000. At 70 km 24 hours after the particles have been removed nitrogen dioxide is still enhanced by a factor of 4 for the strong particle case and a factor of 2 for the weak ionization case. At 65 km the

corresponding situation gives a factor of 100 enhancement for the strong ionization case and a factor of 40 for the weak ionization case.

Nitric Acid Variation Due to Ionization

The concentration of nitric acid above 60 km is a small part of the total odd nitrogen under conditions when there is no electron precipitation. The largest densities are found at night when there is no photodissociation as shown in Figures 6b and 7b. At 65 km the concentration is a maximum of 200 cm^{-3}. There is a decrease by a factor of 10 for each 5 km of altitude increase. For May at 70 degrees north the maximum HNO_3 occurs at 0500 and the minimum between 1900 and 2000 hours depending on the altitude and amount of water.

As a result of increased ionization nitric acid increases dramatically during particle events. The diurnal variation of HNO_3 under the action of particles is shown. There is nitric acid enhancement at both 65 and 70 km. At 70 km the ionization yields as much as several parts per billion nitric acid. There is still substantial nitric acid enhancement 24 hours after particle influx has ceased.

Discussion

The results presented here predict that during particle events nitric oxide will increase at altitudes below 75 km. At this altitude and to an altitude of 90 km or so nitric oxide will not increase during electron events. This is a consequence of the enhanced N , which because of the falloff in molecular oxygen density with altitude has a lifetime which increases with altitude. In fact the present calculations show an NO decrease. The rate of decrease is proportional to the ionization rate. This follows from the fact that the N concentration during an extended event reaches saturation and can be described by photochemical equilibrium, where the N production is proportional to the ionization rate and the loss rate is proportional to the O_2 concentration. Nitric oxide can be increased by shortening the N lifetime.

One mechanism is to cause N to react at a faster rate with O_2. If all N is formed in the ^2D state, the reaction rate will be 1.8×10^8 times faster at 80 km, where the temperature is 180°K, than if it is in the ^4S state. Based on theory and laboratory studies not all N can be placed in the ^2D state. The $N(^4S)$ produced by secondary electrons from ionization during electron events has extrathermal energy, the first few collisions of N with O_2 will produce NO at a rate corresponding to the elevated temperature equivalent to the N energy. There are a number of reactions which lead to elevated energy N. The energy of the nonthermal N is in the range of 0.6 to 2 eV. Based on the computations of Swaminathan et al. [1998] applied to 80 km, this should transfer 30% of the N into reacting with O_2 at an

elevated temperature so that the proportion of $N(^2D)$ as given by Porter et al.[1976] increases from 0.66 to 0.82. This justifies the assumption made by Rusch et al., [1981] in their $N(^2D)$ equal 0.88 case.

An observation of nitric oxide during an electron precipitation event for which mesospheric and lower thermospheric NO was measured has been presented by Crowley et al.,[1998]. The particle fluxes responsible for the ionization were also measured at the same time and fluxes are comparable to the 20 May event. Figure 8 shows the results of UARS HALOE measurements together with the time history of the precipitated fluxes as well as the variation of K_p as presented by Crowley et al. [1998]. The nitric oxide change at different pressure levels is shown over the course of several days during which there was an influx of energetic electrons as shown in the top panel. Nitric oxide increases are observed to coincide with particle flux increases on November 4 for pressure levels corresponding to altitudes at 90 km and above. For the pressure levels at pressures of $5.0x10^{-03}$ (85 km) and $1.0x10^{-2}$ mbar (80 km) there is certainly no increase and in fact a small decrease can be seen at the beginning of 4 November when the particle fluxes maximize.

Conclusions

Large mesospheric nitric oxide increases occur at altitudes below 75 km during electron precipitation events. Nitric oxide increases are accompanied by increases in both nitrogen dioxide and nitric acid. Between 75 and 85 km although N increases dramatically, nitric oxide exhibits strong decline when precipitation exceeds an hour. Net odd nitrogen is increased even though NO decreases. The NO deficit is maintained for at least 24 hours after the particle event ceases. This deficit will be made up by diffusion from the excess NO regions above and below the upper mesosphere. The lack of enhancement in the upper mesosphere is supported by UARS/HALOE measurements of NO during an electron precipitation period. Extra thermal nitrogen probably speeds the conversion of N to NO at altitudes to at least as low as 80 km. The present study shows that the assumption that all N produced by ionization can be treated as NO is incorrect. Such an assumption overestimates the odd nitrogen available to be transported to the stratosphere. The enhanced N in the mesosphere acts as a sink for NO transported from the lower thermosphere. The problem of mesospheric and lower thermospheric odd nitrogen contributions to the stratospheric odd nitrogen budget needs to be addressed with a multidimensional model that includes ion chemistry.

References

Aikin, A. C., and H. J. P. Smith, Mesospheric constituent variations during electron precipitation events, *J. Geophys. Res.*, to be published, 1999.

Baker, D. N., J. B. Blake, D. J. Gorney, P. R. Higbie, R. W. Klebesadel, and J. H. King, Highly relativistic electrons and their influence on the middle atmosphere, *Geophys. Res. Lett.*, *14*, 1027-1030, 1987.

Callis, L. B., and J. D. Lambeth, NO_y formed by precipitating electron events in 1991 and 1992: Descent into the stratosphere as observed by ISAMS, *Geophys. Res. Lett.*, *25*, 1875-1878, 1998.

Crowley, G., A. Ridley, D. Winningham, R. Frahm, J. Sharder, and J. Russell III, Nitric oxide variation in the mesosphere and lower thermosphere during the November 1993 storm period, *J. Geophys. Res.*,*103*, 26,395-26,407, 1998.

DeMore, W. B., et al., Chemical kinetics and photochemical data for use in stratospheric modeling, *JPL Publication 97-4*, 1997.

Frahm, R. A., et al. The diffuse aurora: A significant source of ionization in the middle atmosphere, *J. Geophys. Res.*, *102*, 28,203-28,214, 1997.

Gaines, E. E., D. L. Chenette, W. L. Imhof, C. H. Jackman, J. D. Winningham, Relativistic electron fluxes in May 1992 and their effect on the middle atmosphere, *J. Geophys. Res.*, *100*, 1027-1033, 1995.

Green, B. D., G. E. Caledonia, W. A. M. Blumberg, and F. H. Cook, Absolute production rates and efficiencies of NO in electron-irradiated N_2/O_2 mixtures, *J. Chem. Phys.*,*80*, 773-778, 1984.

O'Keefe, A., G. Mauclaire, D. Parent, and M. T. Bowers, Product energy disposal in the reaction $N^+(^3P)$ with $O_2(X^3\Sigma)$, *J. Chem. Phys.*, *84*, 215-219, 1986.

Porter, H. S., C. H. Jackman, and A. E. S. Green, Efficiencies for production of atomic nitrogen and oxygen by relativistic proton impact in air, *J. Chem. Phys.*, *65*, 154-167, 1976.

Rosenberg, T. J., L. J. Lanserotti, D. K. Bailey, and J. D. Pierson, Energy spectra in relativistic electron precipitation events, *J. Atmos. Terr. Phys.*, *34*, 1977-1990, 1972.

Rusch, D. W., J.-C. Gerard, S. Solomon, P. J. Crutzen, and G. C. Reid, The effect of particle precipitation events on the neutral and ion chemistry of the middle atmosphere, I. Odd nitrogen, *Planet. Space Sci.*, *29*, 767-774, 1981.

Scheibe, M., The increased attachment due to ionization-induced smog in EMP environments, Report Number MRC-R-532, Mission Research Corporation, 1979.

Swaminathan, P. K., et al., Nitric oxide abundance in the mesosphere/

lower thermosphere region: Role of solar soft X-rays, superthermal $N(^4S)$ atoms, and vertical transport, *J. Geophys. Res.*, *103*, 11,579-11,594, 1998.

Umemoto, H., T. Asai, H. Hashimoto, and T. Nakae, Reactions of $N(^2D)$ with H_2O and D_2O; Identification of the two exit channels, NH(ND) + O, *J. Phys. Chem., A*, *103*, 700-704, 1999.

Vitt, F. M., and C. H. Jackman, A comparison of sources of odd nitrogen production from 1974 through 1993 in the Earth's middle atmosphere as calculated using a two-dimensional model, *J. Geophys. Res.*,*101*, 6729-6739,1996.

Zinn, J., and C. D. Sutherland, The solar flare of August 18, 1979: Incoherent scatter radar data and photochemical model comparisons, *J. Geophys. Res.*, *95*, 16,705-16,718, 1990.

Figure Captions

Figure 1 Odd nitrogen reactions

Figure 2 a) Nitric oxide behavior at 65 km. .... curve represents no particle case. ---- curve represents particle fluxes representative of 20 May 1992. _____ curve represents particle fluxes representative of the diffuse aurora situation. b) Atomic nitrogen behavior at 65 km. Curve labeling is the same as panel a.

Figure 3 a) Nitric oxide behavior at 70 km. .... curve represents no particle case. ---- curve represents particle fluxes representative of 20 May 1992. _____ curve represents particle fluxes representative of the diffuse aurora situation. b) Atomic nitrogen behavior at 70 km. Curve labeling is the same as panel a.

Figure 4 a) Nitric oxide behavior at 75 km. .... curve represents no particle case. ---- curve represents particle fluxes representative of 20 May 1992. _____ curve represents particle fluxes representative of the diffuse aurora situation. b) Atomic nitrogen behavior at 75 km. Curve labeling is the same as panel a.

Figure 5 a) Nitric oxide behavior at 80 km. .... curve represents no particle case. ---- curve represents particle fluxes representative of 20 May 1992. _____ curve represents particle fluxes representative of the diffuse aurora situation. b) Atomic nitrogen behavior at 80 km. Curve labeling is the same as panel a.

Figure 6 a) Nitrogen dioxide behavior at 65 km. .... curve represents no particle case. ---- curve represents particle fluxes representative of 20 May 1992. _____ curve represents particle fluxes representative of the diffuse aurora situation. b) Nitric acid behavior at 65 km. Curve labeling is the same as panel a.

Figure 7 a) Nitrogen dioxide behavior at 70 km. .... curve represents no particle case. ---- curve represents particle fluxes representative of 20 May 1992. _____ curve represents particle fluxes representative of the diffuse aurora situation. b) Nitric acid behavior at 70 km. Curve labeling is the same as panel a.

Figure 8 Running average UARS/HALOE NO measurements shown at different pressure levels during a November 1993 electron precipitation event. The top panel gives the incoming electron fluxes as a dashed line. The solid line represents the Kp index. (Adopted from Crowley, 1998).

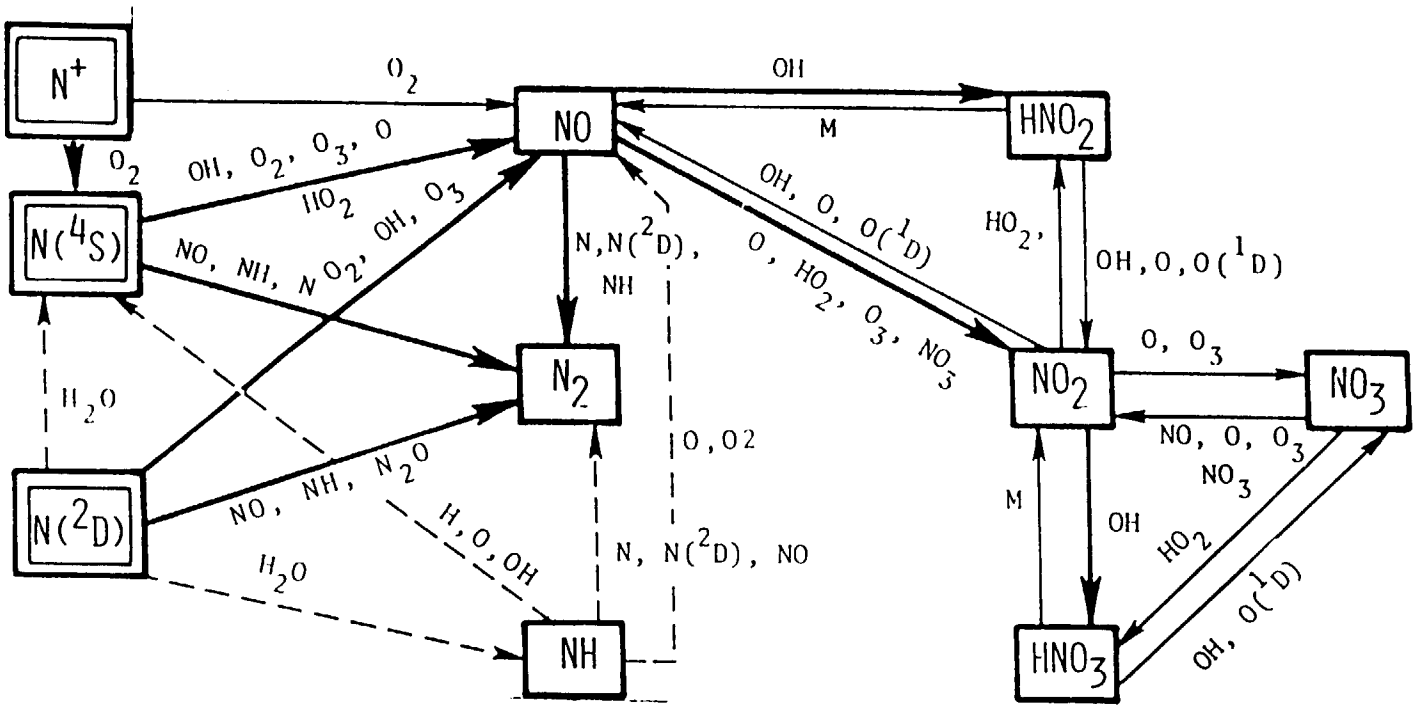

Figure 1 Odd nitrogen reactions

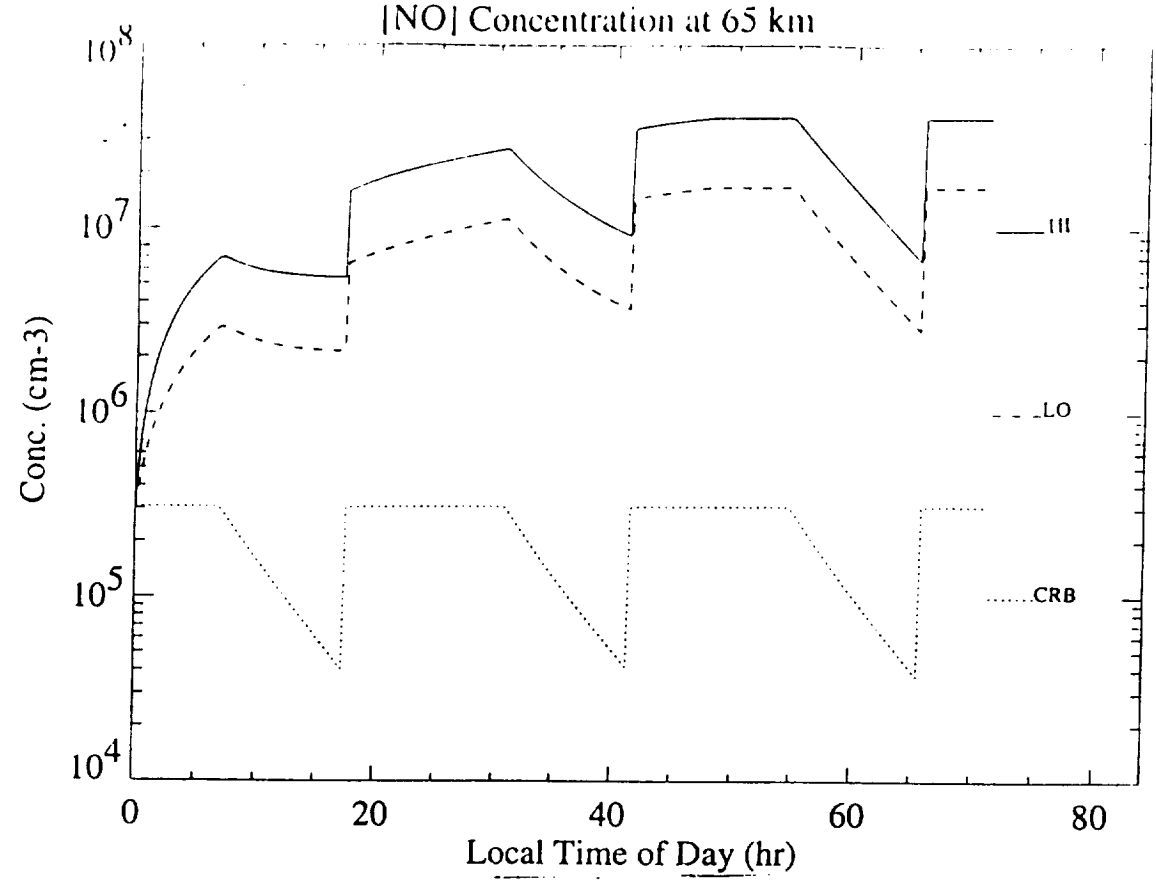

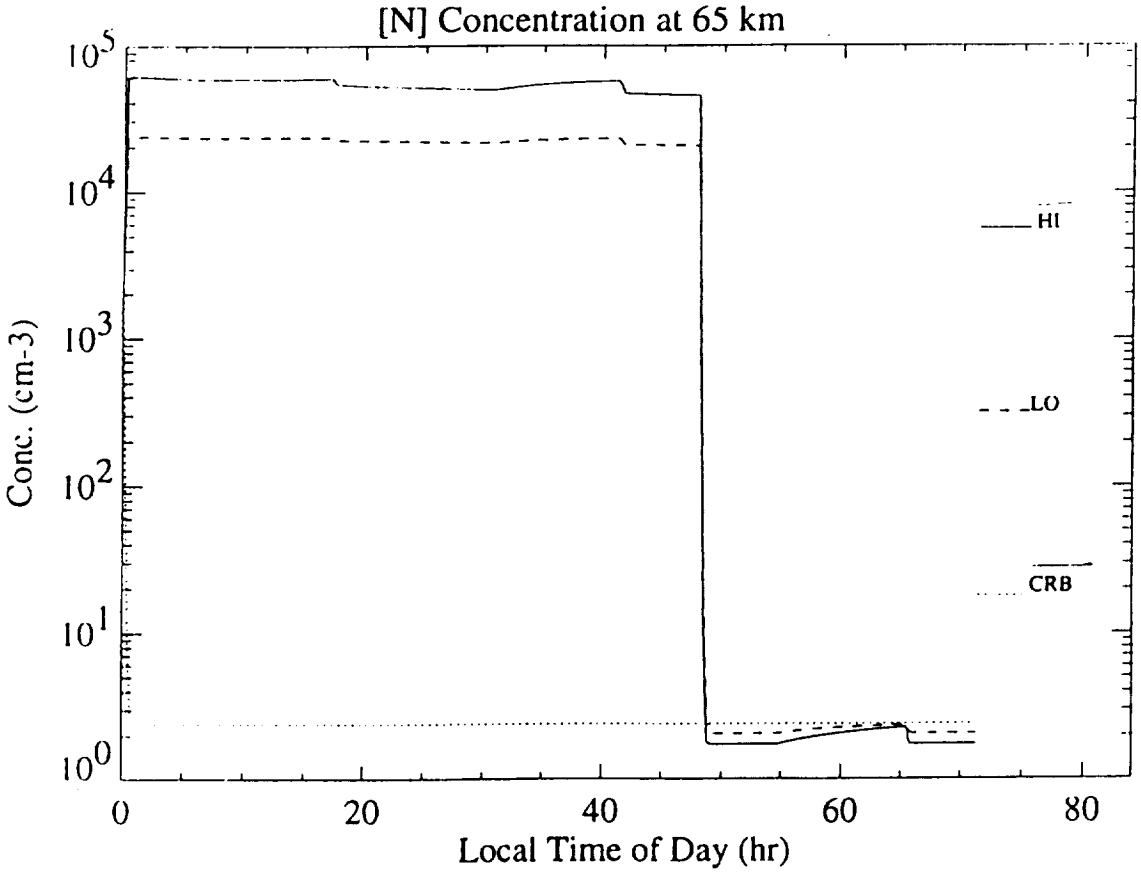

Figure 2 a) Nitric oxide behavior at 65 km. .... curve represents no particle case. ---- curve represents particle fluxes representative of 20 May 1992. _____ curve represents particle fluxes representative of the diffuse aurora situation. b) Atomic nitrogen behavior at 65 km. Curve labeling is the same as panel a.

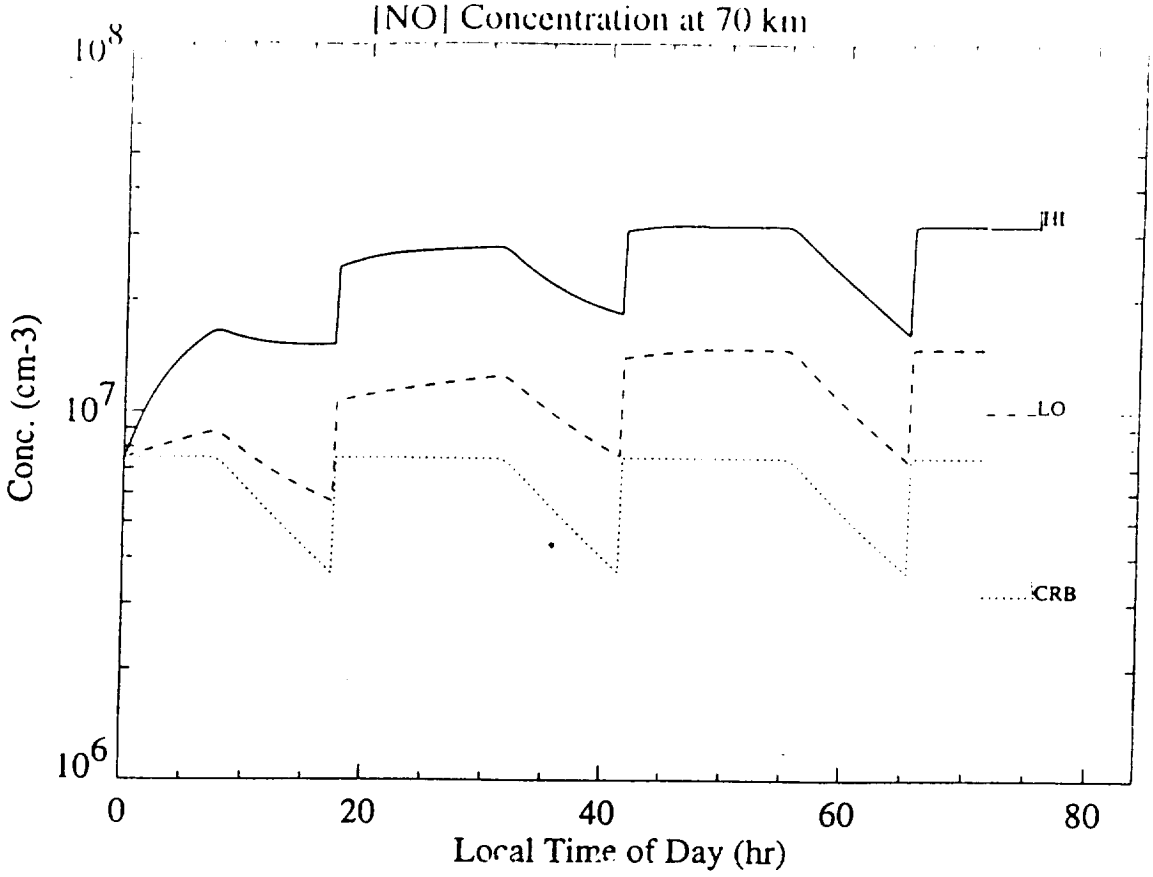

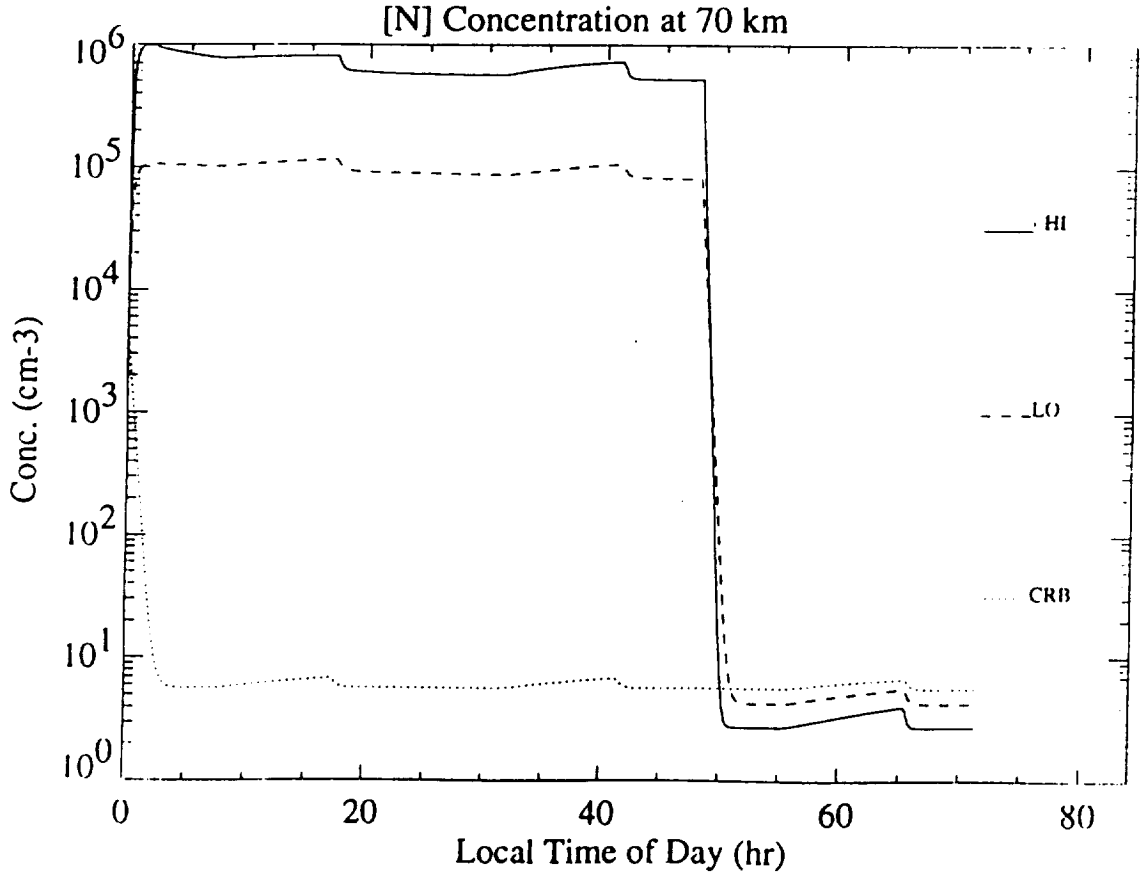

Figure 3 a) Nitric oxide behavior at 70 km. .... curve represents no particle case. ---- curve represents particle fluxes representative of 20 May 1992. _____ curve represents particle fluxes representative of the diffuse aurora situation. b) Atomic nitrogen behavior at 70 km. Curve labeling is the same as panel a.

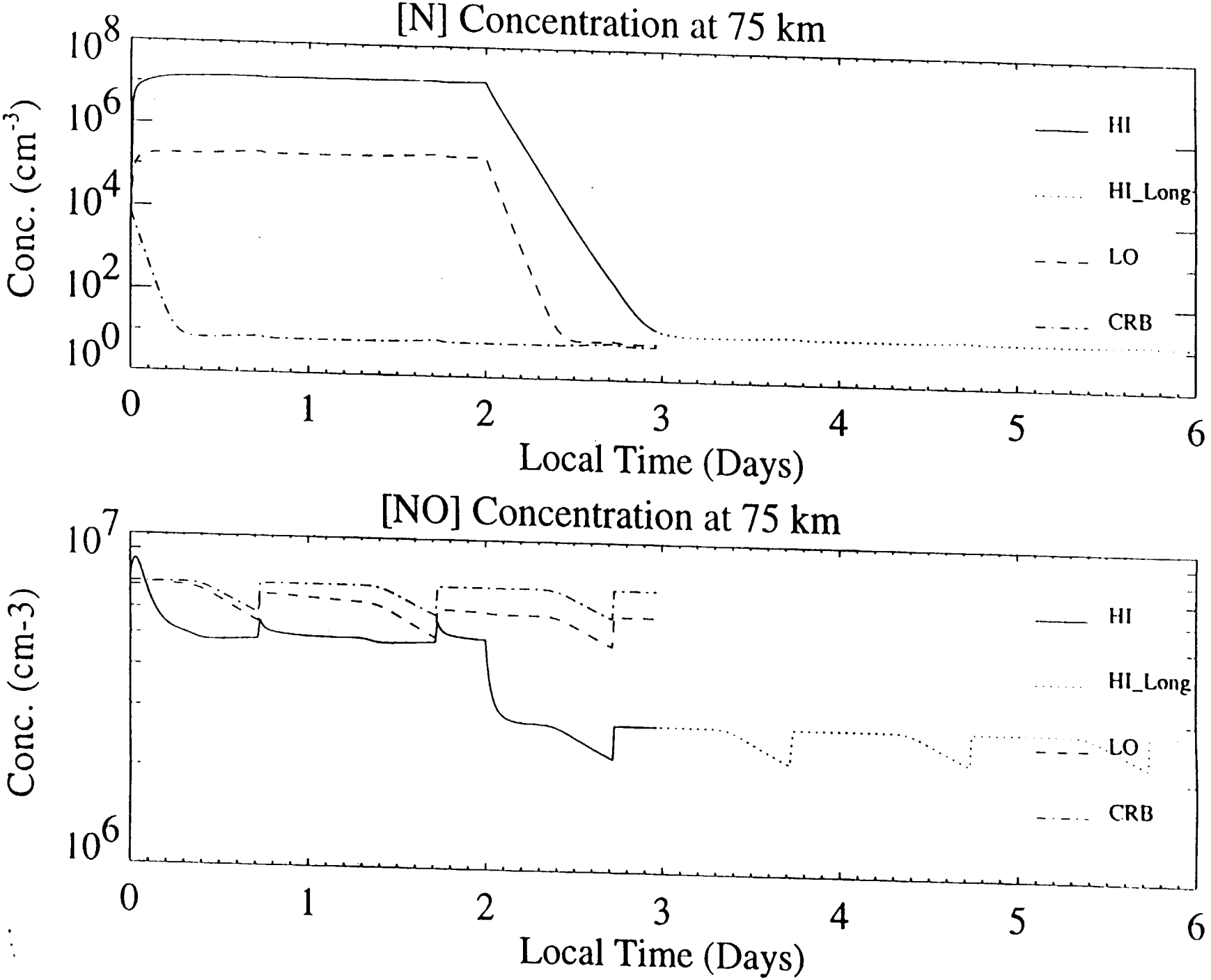

Figure 4 a) Nitric oxide behavior at 75 km. .... curve represents no particle case. ---- curve represents particle fluxes representative of 20 May 1992. _____ curve represents particle fluxes representative of the diffuse aurora situation. b) Atomic nitrogen behavior at 75 km. Curve labeling is the same as panel a.

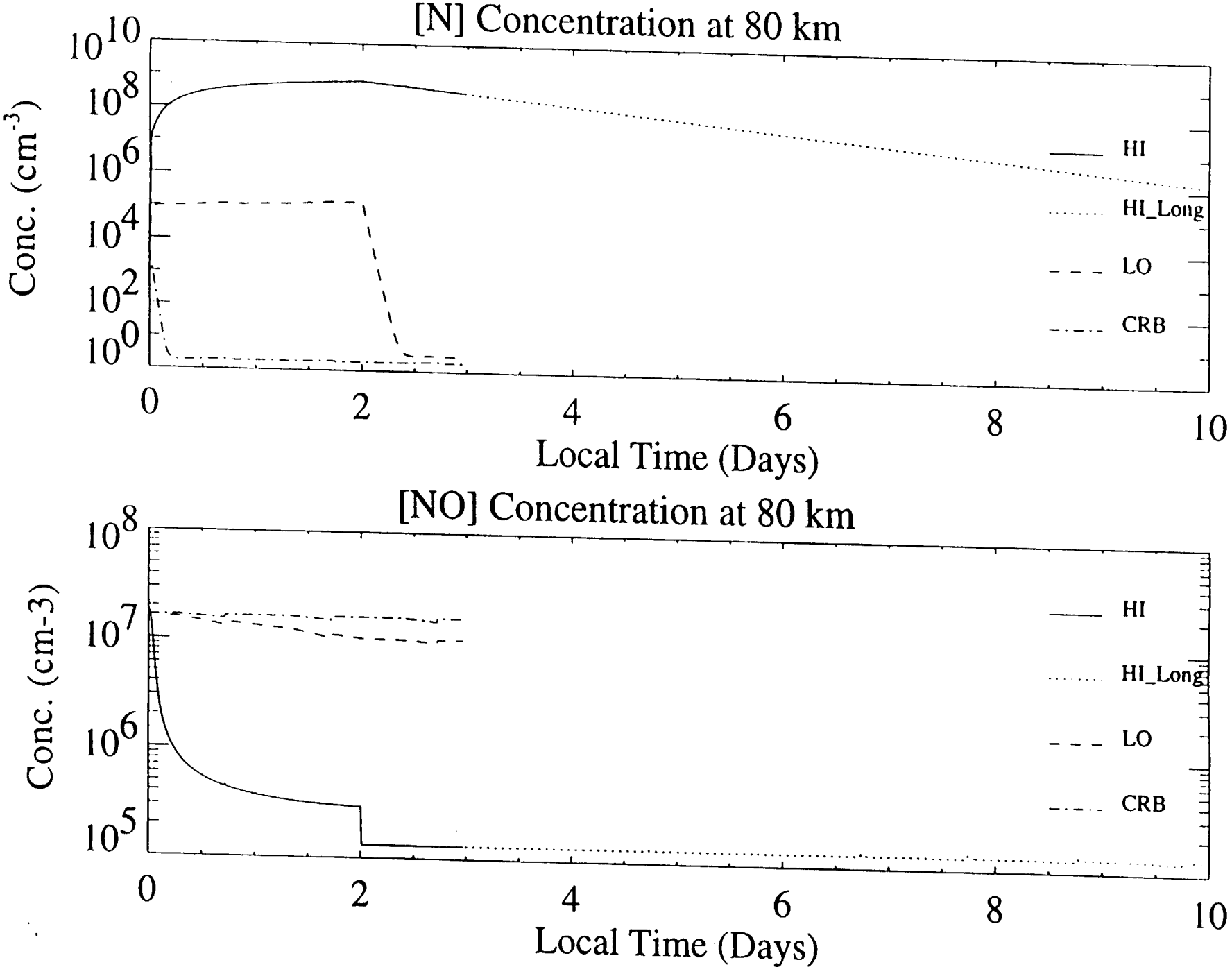

Figure 5 a) Nitric oxide behavior at 80 km. .... curve represents no particle case. ---- curve represents particle fluxes representative of 20 May 1992. _____ curve represents particle fluxes representative of the diffuse aurora situation. b) Atomic nitrogen behavior at 80 km. Curve labeling is the same as panel a.

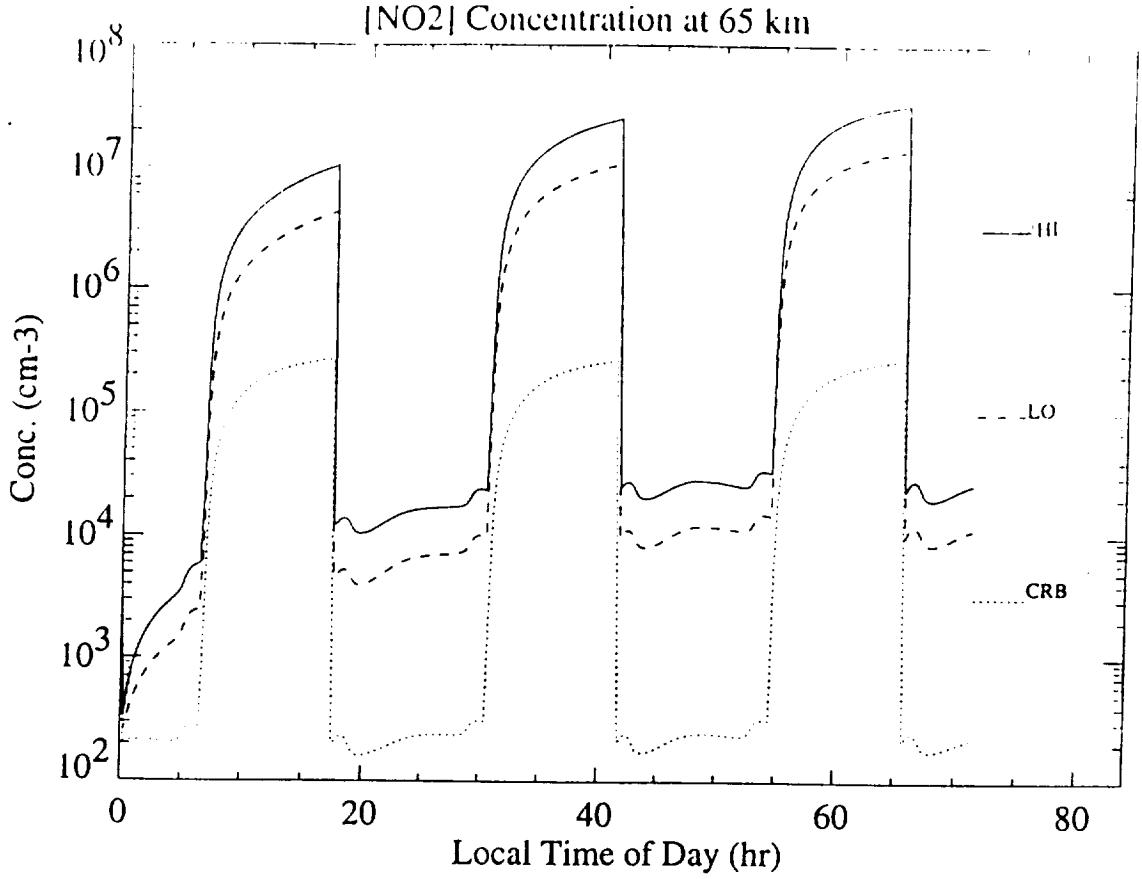

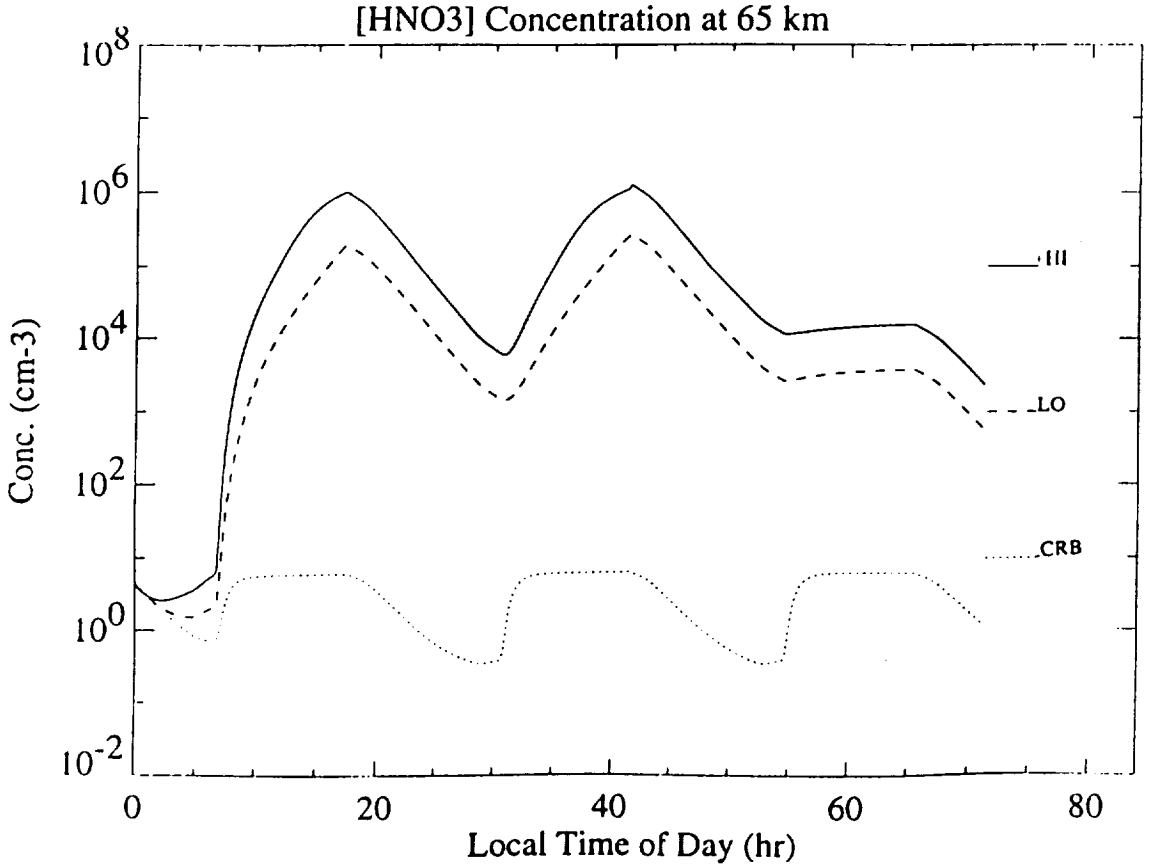

Figure 6 a) Nitrogen dioxide behavior at 65 km. .... curve represents no particle case. ---- curve represents particle fluxes representative of 20 May 1992. _____ curve represents particle fluxes representative of the diffuse aurora situation. b) Nitric acid behavior at 65 km. Curve labeling is the same as panel a.

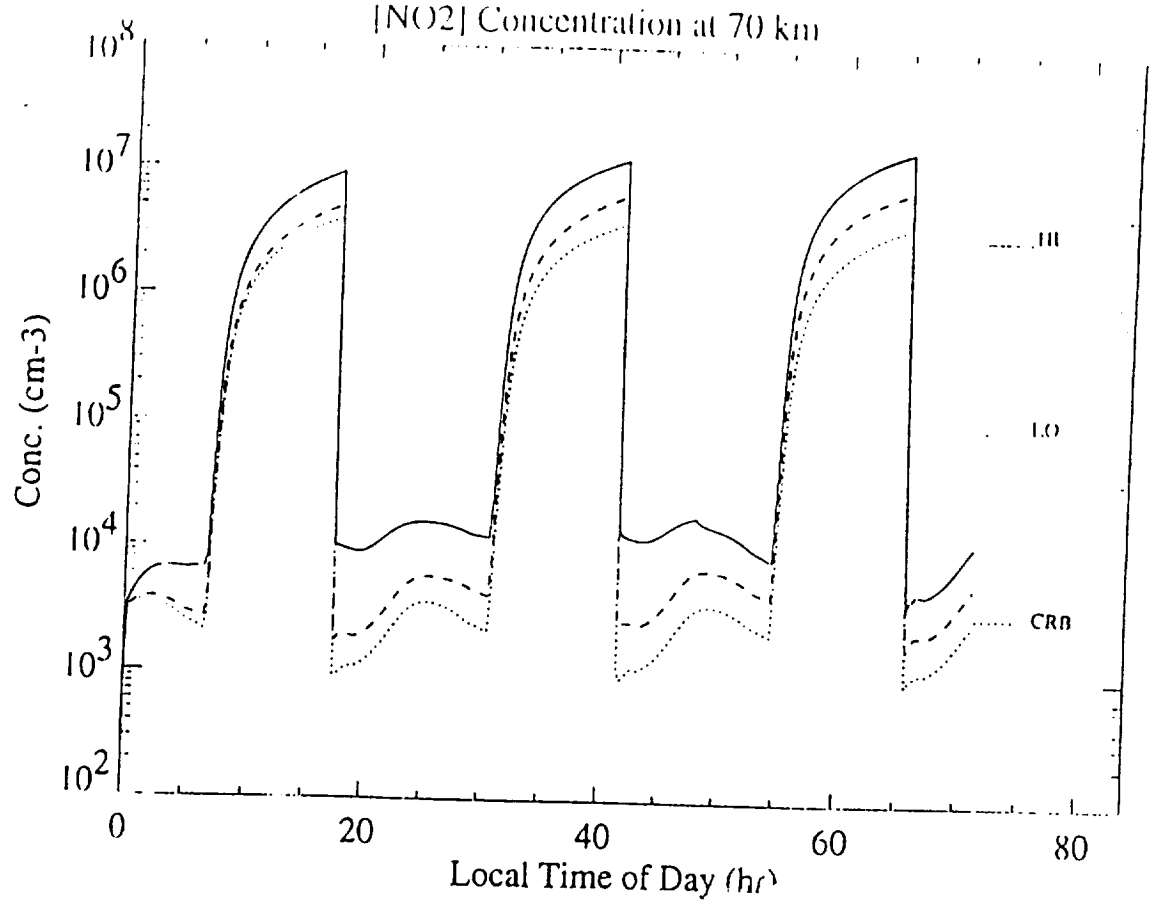

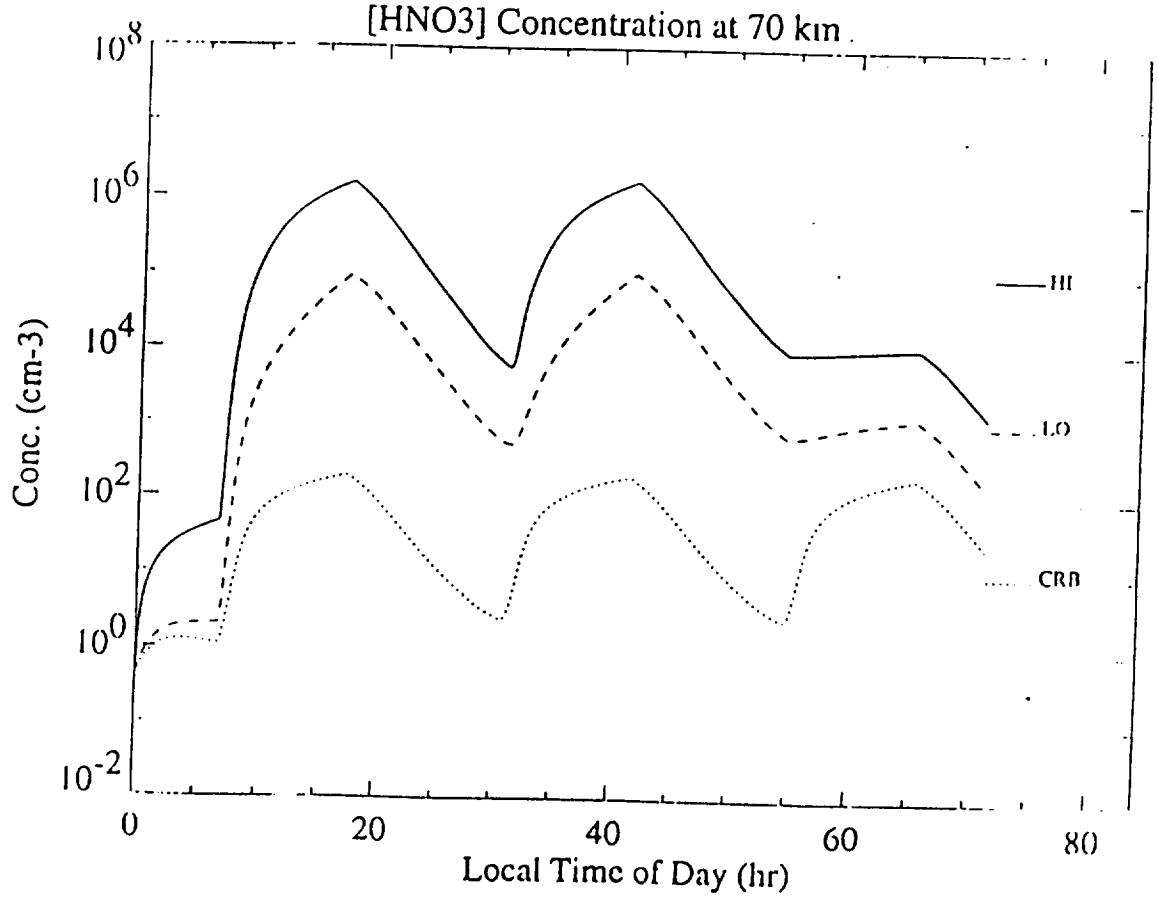

Figure 7 a) Nitrogen dioxide behavior at 70 km. .... curve represents no particle case. ---- curve represents particle fluxes representative of 20 May 1992. _____ curve represents particle fluxes representative of the diffuse aurora situation. b) Nitric acid behavior at 70 km. Curve labeling is the same as panel a.

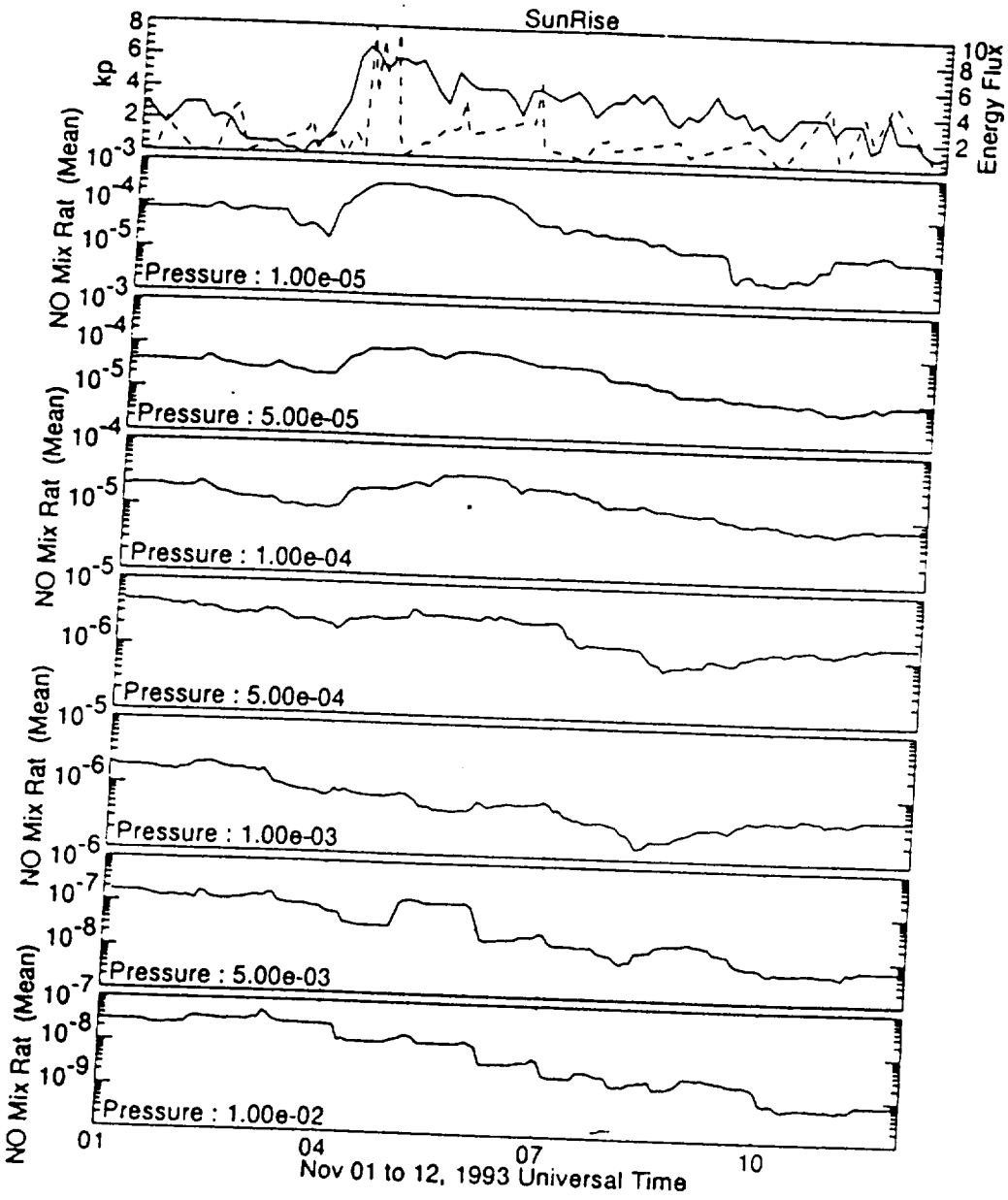

Figure 8 Running average UARS/HALOE NO measurements shown at different pressure levels during a November 1993 electron precipitation event. The top panel gives the incoming electron fluxes as a dashed line. The solid line represents the Kp index. (Adopted from Crowley, 1998).